International Journal of Trend in Scientific Research and Development (IJTSRD)
Volume 4 Issue 3, April 2020 Available Online: www.ijtsrd.com e-ISSN: 2456 – 6470

Geochemical Fractionation of Lanthanides in Stream Sediments around Bwanebwa Area, Pan-African Fold Belt (Cameroon)

Ndema Mbongué Jean-Lavenir[1,2]

[1]Department of Geology, University of Buea, Buea, Cameroon
[2]Laboratory of Petrology and Structural Geology, Department of Earth Sciences, Faculty of Sciences, University of Yaoundé I, Yaounde, Cameroon

ABSTRACT

Fifteen stream sediment samples were collected in Bwanebwa area, situated southwestern part in the central domain of the Pan-African Fold Belt in Cameroon. Samples were analyzed by Aqua Regia - Inductive Coupled Plasma - Mass Spectrometry analytical technique. The chemical analyses revealed a wide variability of lanthanide concentrations (ΣREE = 1471.56-7674.2 ppm) displaying a normal distribution pattern. Lanthanides show a high enrichment in La, Ce, Pr, Nd, and the proportion enrichment of REEs is still similar with increasing atomic number. The order of the average concentrations of REEs is Ce > La > Nd > Pr > Sm > Gd > Dy > Er > Tb > Ho >Yb > Eu > Tm > Lu, which was different to that found in the Oddo-Harkins rule, earth's crust, upper continental crust, South China Sea, mean REE values in oceanic crust, Redang Island Marine Sediment in Terengganu Coastal Waters, Bayan Obo ores, Edéa, suggesting that REEs set up a complex group. The LREE/HREE ratio (31.57-35.24, av. = 32.82) showed that the content of LREE (1425-7449.8, av. = 3699) is significantly higher than that of HREE (46.56-224.4, av. = 112.07). LREEs account for 97.06% of the total REEs and this percentage is in agreement with the trend that was observed in the earth's crust and in the Bayan Obo ores. Chondrite-normalized REE distribution patterns are identical, indicating the consistency of geochemical distribution of REEs in stream sediments. They are strongly fractionated, with LREEs significantly fractionated (La_N/Yb_N = 11.74-27.93, av. = 21.04) relative to HREEs (Gd_N/Yb_N = 7.40-16.69, av. = 13.35), implying that HREEs are more soluble and more complex than middle or LREE and are more strongly absorbed on most substrates. Positive Ce anomaly (Ce/Ce* = 1.04-1.07) and negative Eu anomaly (Eu/Eu* = 0.097-0.17) were observed, indicating that differentiation occurred between Ce, Eu and other lanthanides. Therefore the positive Ce anomaly recorded represents an enrichment of Ce compared with its neighboring elements. A five-factor model of the REEs that accounts for 1.998% of the total data cumulative variance have been observed, with the communality values (0,996-1) reflecting stronger community structure. Principal component analysis results in five components that explain 100% of the total variance, with the placement of elements in three major principal components, in which elements scattering in the rotated space displaying their mutual association. The results provide evidence for similar input sources and common geochemical characteristics of REEs. Lanthanide concentrations in Bwanebwa area were of geogenic origins and not influenced by anthropogenic sources. The abundance of REEs is related to the lithology made up of granites and associated pegmatites. Cerium shows the highest average content of REEs, followed by La, Nd, Pr, Gd, Sm, hence pattern of Ce distribution shows higher than the other lanthanides. LREEs (La, Ce, Pr, Nd) and Ga fall above the upper background threshold limit and are considered as anomalous. Therefore the results of this work serve as guide for lanthanides exploration in Bwanebwa area.

KEYWORDS: *Bwanebwa area; Lanthanide concentrations; Oddo-Harkins rule; complex group; stronger community structure; geogenic origins; upper background threshold*

How to cite this paper: Ndema Mbongué Jean-Lavenir "Geochemical Fractionation of Lanthanides in Stream Sediments around Bwanebwa Area, Pan-African Fold Belt (Cameroon)" Published in International Journal of Trend in Scientific Research and Development (ijtsrd), ISSN: 2456-6470, Volume-4 | Issue-3, April 2020, pp.363-373, URL: www.ijtsrd.com/papers/ijtsrd30430.pdf

IJTSRD30430

1. INTRODUCTION

Rare earth elements (REEs) include a series of lanthanide (Ln) elements, the elements with atomic numbers 57 to 71; and they have similar electronic structures and chemical properties. Because scandium (Sc) and yttrium (Y) exhibit similar properties to the lanthanide family, they are also considered rare earth elements [1]. Two to three groups of

REEs are generally distinguished into light rare earth elements (LREEs), heavy rare earth elements (HREEs), and sometimes middle rare earth elements (MREEs) based on their atomic mass and effective ion radius [2] and [3]. The LREEs or elements of the cerium subgroup are the lower atomic weight elements, (atomic mass less than 153 g/mol and ionic radius > 95 pm). This subgroup includes elements from lanthanum to europium. The HREEs or elements of the yttrium subgroup with atomic mass above 153 g/mol, encompass lanthanides from gadolinium to lutetium, including yttrium, which is similar in its chemical properties and whose mass is equal to 88.9 g/mol [4]. Sm to Ho are the elements of the MREEs. REEs generally occur as trivalent ions, Ce can be also in tetravalent state, and Eu is in divalent state.

Lanthanides are highly electropositive and are predominantly trivalent (Ln^{3+}), with the exception of cerium (Ce^{4+}) and europium (Eu^{2+}) in some environments. The entry of new electrons in the 4f orbitals, when the atoms have fully occupied the 6s orbital increases the electrostatic attraction between the N shell and the nucleus. This leads to a reduction of the REE^{3+} ionic radius with increasing Z, a phenomenon which is known as lanthanide contraction [5] and [6]. Since most Ln possess similar atomic radii and oxidation states, they can substitute for each in various crystal lattices. This capability of substitution leads to multiple REE occurrences within a single mineral and has resulted in a wide distribution within the Earth's crust [7]. REEs are found in a wide range of mineral types, including halides, carbonates, oxides, phosphates and silicates. The abundance of lanthanides within Earth's crust varies widely across individual REEs, ranging from the most abundant at 66 ppm of cerium (exceeding other important metals including copper: 27 ppm and lead: 11 ppm) to 0.28 ppm for thulium [8] and [9].

During the last few decades, REEs have become important geochemical tracers in order to understand and describe the chemical evolution of the earth's continental crust [10]-[13]. Rare earth elements have been used, as analogues for actinide elements, in studies related to radioactive waste disposal in order to demonstrate their general immobility in weathering environments [14]. The comparison among REE facilitates the normalization of analyses to reference standards such as chondrite [15]. Technological developments have increased the use of REE in the defense, aerospace, medical and automotive industries. Lanthanides are essential components of catalysts, high-strength magnets, super-alloys, display technology and lasers [10], [16], [17]. Their concentration has been proven to occur in a wide range of geological settings [18], [19].

World resources of lanthanides are contained primarily in the minerals bastnäsite, monazite, loparite, and in ion-adsorption clays [20]. Bastnäsite deposits in alkaline rocks and carbonatites of China and the United States constitute the largest percentage of the world's economic resources, while monazite deposits in Australia, Brazil, China, India, Malaysia, South Africa, Sri Lanka, Thailand, and the United States make up the second largest segment [21]. Brazilian deposits account for about 1% of the world reserve [22]. Currently, the use of REEs is closely associated with high-tech industry. The increasing use of REEs in industrial processes suggests that REEs release into the environment is likely to increase in the future with potential impacts on human health [23].

Despite vast global distribution, REEs are mainly mined in China. In 2011, China produced over 90% of the world's rare earth supply while owning only 23% of the world's total reserves [24]. Due to the increase of rare earth mineral mining, China's rare earth reserve has drastically decreased from 75% in 1970 to 23% in 2011 [25] and [24]. The surface mining and heap leaching of China's unique ion-adsorption rare earth resources have caused severe environmental damage, such as soil erosion, pollution, and acidification. Moreover, REEs have long been used in China as additives in fertilizers and as growth promoters in livestock feed. The long-term effects and damage of such uncontrolled discharge of REE-based chemicals into the environment remain to be determined. Lanthanides have been characterized neither as essential elements for life nor as strongly toxic elements in the environment [26]. Although the environmental toxicity of REEs is largely unknown, environmental contamination has already been found in some mineralized areas as well as soils that are affected by the long-term application of sludge. Several negative effects of REEs on organisms have been reported.

Little are known about lanthanides in Cameroon, meanwhile preliminary studies have been done by [27] who reported for the first time the distribution of rare earth elements from the metamorphic rocks of the Paleoproterozoic Nyong unit situated at the west of Congo Craton in Cameroon. The present study is carry out in Bwanebwa area situated around the central domain of the Pan-African Fold Belt in Cameroon. The aim of this work is to study the chemical distribution and fractionation of lanthanides in stream sediments samples collected in Bwanebwa area.

2. Regional Geology

The Bwanebwa region is located in the southwestern part of the central domain of the Pan-African Fold Belt (PAFB) in Cameroon (Fig.1). The PAFB is a major Neoproterozoic Orogen linked to the Trans-Saharan Belt of western Africa and to the Brasiliano Orogen of NE Brazil [28] and [29]. In Cameroon the PAFB is made up of three main domains [30]-[36], (Fig. 1): (1) the southern domain, which corresponds to the northern edge of the Congo Craton, formed by Neoproterozoic metasediments deposited in a passive margin environment and metamorphosed under high pressure conditions at 616 Ma; (2) the northern domain consisting of subordinate 830 Ma old metavolcanic rocks of tholeiitic and alkaline affinities; (3) the central domain that contains the present study area, is situated between the Sanaga shear zone (SSZ) and the Betaré-Oya shear zone (BOSZ) [37] to the south, and the Tibati-Banyo fault (TBSZ) to the north [38]. This domain is dominated by a NE-SW elongated regional-scale plutonic complex intrusive into a Paleoproterozoic basement and locally covered by Cretaceous deposits (Mbere and Djerem basins) and by Cenozoic volcanic rocks of the Cameroon Volcanic Line (CVL). The study area is made up of granites and the associated pegmatites.

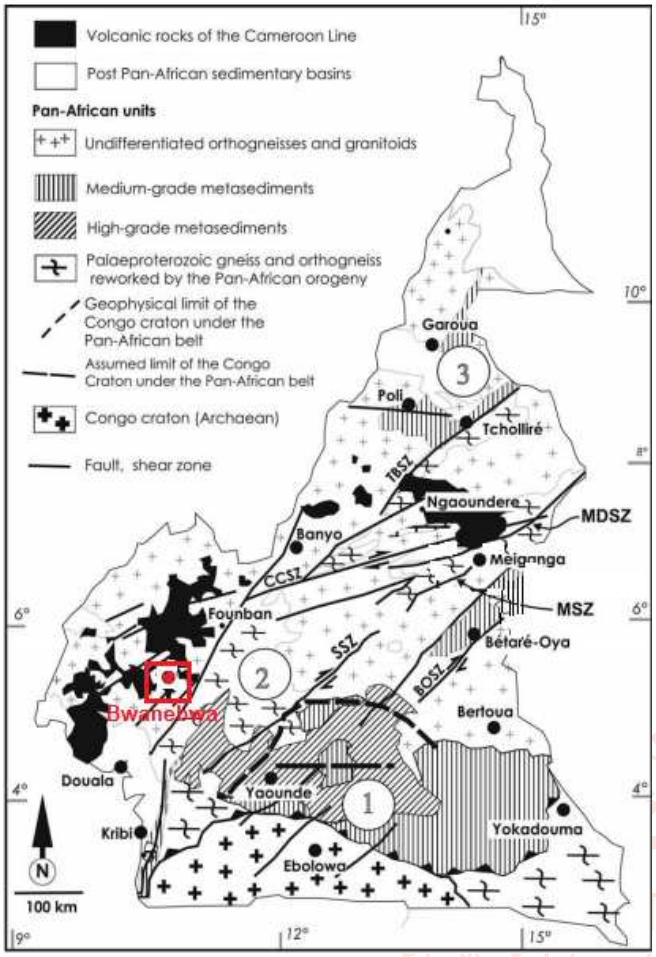

Figure1. Geologic map of Cameroon, modified from [31], [35], [39]-[41], showing major lithotectonic units and shear zones: (1) southern domain; (2) central domain; (3) northern domain; CCSZ, Central Cameroon shear zone; TBSZ, Tcholliré-Banyo shear zone; SSZ, Sanaga shear zone; BOSZ, Betaré- Oya shear zone. The location of the study area is marked by a red box.

3. Methods of investigation

Fifteen stream sediment samples were collected in the study area. Prior to the sampling process, the areas were surveyed, in order to see the favorable sites for sampling. Sampling points are found along the stream banks where the flow velocity is low and favors deposition (area with no limited sediment accumulation). The GPS coordinates of the chosen sites were then taken and recorded on the field notebook. Stream sediment samples were collected downstream at interval of about 300m, at depth of about 30-50cm to avoid high contents of Fe-Mn oxides coating. During the panning process, large particles were removed with the hands. Panning was carefully done for at least 30-45 minutes and the obtained concentrates collected. The collected concentrates were put into polythene bags and labelled. The samples were then air dried, weighed on clean paper sheets to avoid contamination at the geological laboratory of the University of Buea for a period of one week. After drying, about 5g of the bulk samples were packaged and sent to Activation Laboratories (ACTLABS) in Canada for chemical analysis. Chemical analysis was performed on the fifteen stream sediments samples using Aqua Regia - Inductive Coupled Plasma- Mass Spectrometry (AR-ICP-MS) analytical technique.

4. Results

4.1. Geochemical data

The chemical composition of lanthanides of stream sediments from Bwanebwa area is represented in table 1. The chemical analyses revealed a wide variability of REE contents with ΣREE in the range of 1471.56 to 7674.2 ppm with an average of 3811 ppm (Table 1). The overall stream sediment samples show a high enrichment in La (332-1750 ppm, av. = 863.8 ppm), Ce (703-3758 ppm, av. = 1846.93 ppm), Pr (76.11-392 ppm, av. = 196.89 ppm) and Nd (269-1440 ppm, av. = 715.53 ppm). Only samples EB05 and EB07 show relative enrichment in Yb (4.6 and 4 ppm respectively; Table 1). The concentrations of individual REEs tend to decrease with increasing atomic number, REEs with even atomic numbers are more frequent than their neighbors with odd atomic numbers. The order of the average concentrations of REEs in stream sediments around Bwanebwa area is as follows (in decreasing order): Ce>La>Nd>Pr>Sm>Gd> Dy>Er>Tb>Ho>Yb>Eu>Tm>Lu.

The LREE/HREE ratio ranged largely from 31.57 to 35.24 with an average of 32.82. This ratio showed that the content of LREE (1425-7449.8, av. = 3699) is significantly higher than that of HREE (Gd-Lu) that yields between 46.56 and 224.4 with 112.07 as average. The content of LREEs (La-Eu) accounted for 97.06% of the total REEs content in the investigated stream sediments, just as they are in the earth's crust [3]. This percentage is in agreement with the trend observed in the Bayan Obo ores [42].

The distribution of REEs in stream sediments normalized to upper continental crust (UCC) after [9] are illustrated in Fig. 2. The REEs normalized patterns are strongly fractionated (La_N/Yb_N = 11.74-27.93). They show LREEs significant fractionation (La_N/Yb_N = 11.74-27.93, av. = 21.04; Ce_N/Sm_N = 1.12-2.48) relative to HREEs (Gd_N/Yb_N = 7.40-16.69, av. = 13.35). They display a pronounced negative Eu anomaly (Eu/Eu* = 0.097-0.17), a very slightly positive Ce anomaly (Ce/Ce* = 1.04-1.07) and a very weak positive Nd anomaly (Nd/Nd* = 0.97-1.46). Also, REEs distribution patterns are similar and parallel.

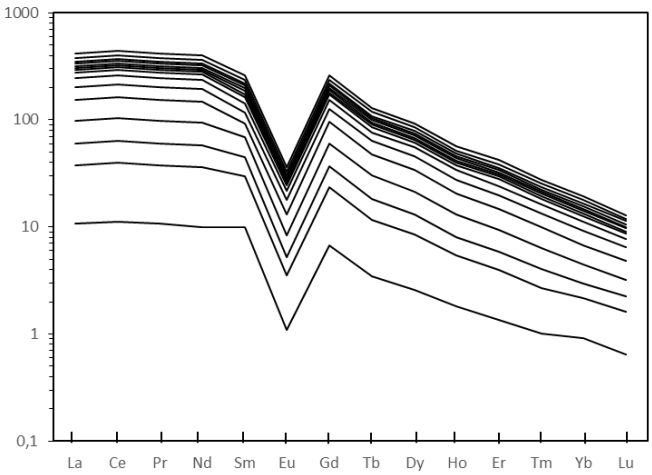

Figure2. Upper continental Crust normalized REE patterns.

TABLE I Lanthanides Characteristics of Stream Sediments from Bwanebwa

REE	EB01	EB02	EB03	EB04	EB05	EB06	EB07	EB08	EB09	EB10	EB11	EB12	EB13	EB14	EB15	Mean
La (ppm)	333	835	710	1159	1753	1522	1350	940	455	405	425	505	440	940	1185	863.8
Ce	703	1792	1503	2492	3758	3290	2879	2010	976	855	927	1062	945	2020	2492	1846.9
Pr	76.11	191	159	265	392	352	308	218	107	91.3	100	115	100	215	264	196.89
Nd	270	704	579	967	1441	1270	1121	794	385	325	362	420	370	775	950	715.53
Sm	41.79	82	66	100	101	102	100	91.9	44.5	48	47.8	49	44.3	81	101	73.35
Eu	1.1	2.4	1.7	3.2	4.8	4.5	4	2.7	1.2	1	1	1.3	1.4	2.6	3.4	2.42
Gd	27.1	66.8	54.73	94	138	124	105	76.8	35.8	34.2	37.3	38.4	36	73	92	68.88
Tb	2.41	5.7	4.7	8.22	12.4	10.9	9.3	6.6	3.1	3.2	3.4	3.3	3.1	6.3	8.1	6.05
Dy	10.12	23.1	17.5	33	49	44.3	38	26.2	12	12.7	13.6	13.2	13	25	32	24.18
Ho	1.5	3	2.2	4.12	6.3	5.9	5	3.4	1.6	1.6	1.8	1.7	1.8	3.1	4.1	3.14
Er	3.1	6	4.3	8.23	12.5	11.4	10	9	3.4	3.2	3.5	3.6	3.7	6.4	8	6.42
Tm	0.3	0.51	0.4	0.7	1.1	1	0.9	0.6	0.3	0.3	0.3	0.3	0.4	0.5	0.7	0.55
Yb	1.83	2.5	1.64	3	4.6	4.8	4	3	1.4	1.5	1.4	1.7	2	2.3	3.1	2.56
Lu	0.2	0.3	0.2	0.3	0.5	0.5	0.4	0.3	0.1	0.2	0.1	0.2	0.2	0.2	0.3	0.27
ΣREE	1471.56	3714.31	3104.37	5137.77	7674.2	6743.3	5934.6	4182.5	2026.4	1782.2	1924.2	2214.7	1960.9	4150.4	5143.7	3811
LREE	1425	3606.4	3018.7	4986.2	7449.8	6540.5	5762	4056.6	1968.7	1725.3	1862.8	2152.3	1900.7	4033.6	4995.4	3699
HREE	46.56	107.91	85.67	151.57	224.4	202.8	172.6	125.9	57.7	56.9	61.4	62.4	60.2	116.8	148.3	112.07
LREE/ HREE	30.61	33.42	35.24	32.90	33.20	32.25	33.38	32.22	34.12	30.32	30.34	34.49	31.57	34.53	33.68	32.82
(La/Yb)N	11.74	21.55	27.93	24.92	24.59	20.46	21.77	20.22	20.97	17.42	19.59	19.17	14.19	26.37	24.66	21.04
(Gd/Yb)N	7.40	13.36	16.69	15.67	15	12.92	13.12	12.8	12.79	11.4	13.32	11.29	9	15.87	14.84	13.35
(Ce/Sm)N	1.12	1.46	1.52	1.66	2.48	2.15	1.92	1.46	1.46	1.19	1.29	1.44	1.42	1.66	1.64	1.59
(La/Sm)N	1.08	1.38	1.46	1.57	2.35	2.02	1.83	1.39	1.39	1.14	1.20	1.40	1.35	1.57	1.59	2.18
Eu/Eu*	0.13	0.13	0.12	0.14	0.17	0.16	0.16	0.13	0.12	0.10	0.10	0.12	0.14	0.14	0.14	0.15
Ce/Ce*	1.04	1.06	1.05	1.06	1.07	1.06	1.05	1.05	1.04	1.05	1.06	1.04	1.06	1.06	1.05	1.43
Nd/Nd*	0.97	1.14	1.14	1.20	1.46	1.36	1.29	1.13	1.13	0.99	1.06	1.13	1.12	1.19	1.18	1.6

TABLE II Description Statistics of Rees Concentration in Stream Sediment from Bwanebwa

REEs	Min	Max	Mode	Range	Mean	GM	Median	Std Dev	CV (%)	Variance	Skewness	Kurtosis	IQR	Q1	Q3	UBT
La	333	1753	940	1420	864	755.85	835	451	52.21	203354	0.57	-0.78	745	440	1185	345.93
Ce	703	3758	2492	3055	1847	1614.44	1792	969	52.45	938341	0.59	-0.75	1547	945	2492	524.79
Pr	76.1	392	100	315.89	196.9	172.68	191	101.8	51.72	10368.4	0.55	-0.86	165	100	265	172.44
Nd	270	1441	-	1171	715.5	626.47	704	371.9	51.98	138343.1	0.56	-0.79	597	370	967	336.5
Sm	41.79	102	100/101	60.21	73.35	69.07	81	25.16	34.3	633.03	-0.09	-1.97	52.2	47.8	100	144.83
Eu	1	4.8	1	3.8	2.42	2.09	2.4	1.316	54.38	1.732	0.55	-1.03	2.2	1.2	3.4	22.46
Gd	27.1	138	-	110.9	68.88	60.59	66.8	35.48	51.51	1258.59	0.6	-0.77	58	36	94	99.96
Tb	2.41	12.4	3.1	9.99	6.049	5.32	5.7	3.151	52.09	9.928	0.68	-0.61	5.02	3.2	8.22	30.2
Dy	10.12	49	-	38.88	24.18	21.28	23.1	12.64	52.27	159.76	0.69	-0.7	20	13	33	58.1
Ho	1.5	6.3	1.6/1.8	4.8	3.141	2.78	3	1.626	51.76	2.644	0.77	-0.6	2.42	1.7	4.12	25.62
Er	3.1	12.5	-	9.4	6,422	5.70	6	3.23	50.3	10.434	0.6	-1.02	5.5	3.5	9	29.07
Tm	0.3	1.1	0.3	0.8	0.554	0.50	0.5	0.2721	49.11	0.074	0.86	-0.45	0.4	0.3	0.7	5.48
Yb	1.4	4.8	1.4/3	3.4	2.585	2.37	2.3	1.141	44.16	1.303	0.85	-0.41	1.46	1.64	3.1	19.92
Lu	0.1	0.5	0.2	0.4	0.2667	0.24	0.2	0.1234	46.29	0.0152	0.74	-0.03	0.1	0.2	0.3	66.14

GM: Geometric mean; Std Dev: Standard deviation; CV: Coefficient of variation or relative standard deviation (RSD); IQR: Interquartile range;
Q1: First quartile; Q3: Third quartile; UGT: Upper Background Threshold

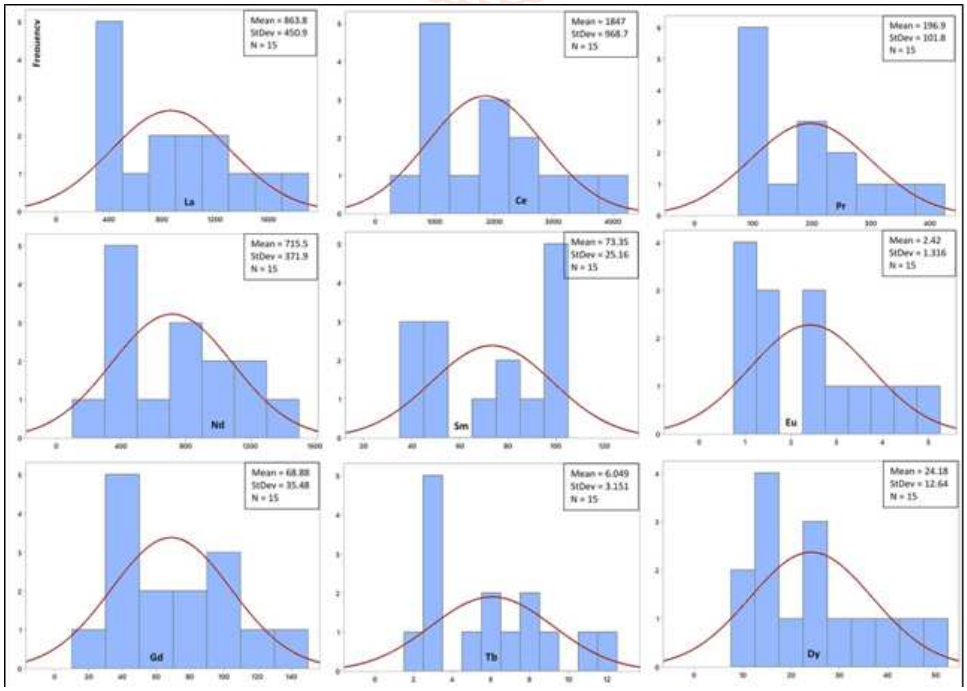

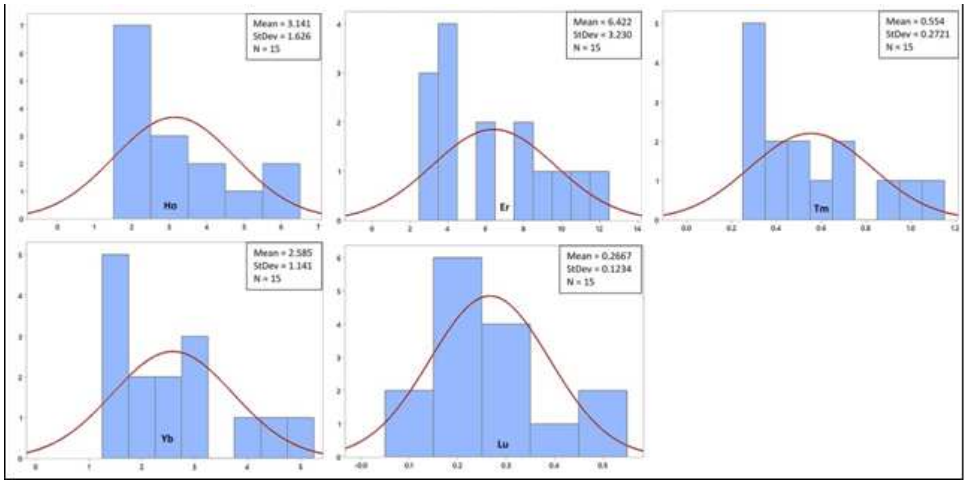

Figure3. Cumulative Frequency Plots of Rare Earth Elements

4.2. Data distribution patterns

Table 2 presents the descriptive statistics of lanthanides in stream sediments. A summary of the main statistical parameters (mean, range, median, and standard deviation) was also shown. The geometric mean (GM) were used to describe the average concentrations [43]. The stream sediments content the LREEs (La, Ce, Pr, Nd, Sm, Eu) and the HREEs (Gd, Tb, Dy, Er, Y, Lu). They are characterized by high abundance of Ce (703-3758 ppm), La (333-1753 ppm), Nd (269-1440 ppm), relative abundance of Pr (76.11-392 ppm), and depletion of HREEs. The average values (GM) are closer to the median values for all the REEs indicating a symmetric data distribution pattern REE (Table 2). Moreover, the very low positive skewness values suggest that individual REE datasets were very weakly right-skewed model. Also, the very low negative kurtosis values indicate a very slightly light-tailed distribution. However, the studied REEs still follow a normal distribution. The graphical inspection of original data distribution for all REEs shows a clear normal distribution (Fig. 3). The standard deviation values were high for some elements, particularly for LREEs (La to Nd), and Gd (Table 2). The coefficient of variation (CV) or the relative standard deviation (RSD) can be used to compare in relative terms the variability of the same property under similar values of variance and different means. Low CV values correspond to a spatially homogeneous distribution of REE concentrations, whereas high CV values indicate a non-homogenous surface distribution [44]. The relative standard deviation values are moderate for the studied lanthanides, greater to 50% (Table 2), indicating a moderate variability. The spatial variability of Sm, Tm, Yb and Lu, however, was low with the CVs only fluctuating from 34.3 to 49.11%.

4.3. Multivariate statistical analysis (MSA)

In an attempt to identify REE associations, Pearson's correlation matrix and factor analysis was carried out to investigate the inter-element relationship. The analysis factors related variables into principal associations on the basis of their mutual correlation coefficients [45].

4.3.1. Correlation analysis

The correlation analysis (Table 3) between REEs exhibits an unusually case where all the REEs display higher positive correlation (r = 0.9144-0.9998) with their respective correspondents. Only correlation values between Sm and Tm, Yb and Lu that are slightly low with r values ranged from 0.8235 to 0.8885. These findings provide evidence for similar input sources and common geochemical characteristics of the elements.

4.3.2. Factor Analysis

Table 4 shows a five-factor model of the REEs that accounts for 1.998% of the total data cumulative variance. Factor 1 (La, Ce, Pr, Nd, Eu, Gd, Tb, Dy, Ho, Er, Tm, Yb, Lu) account for 0.363% of the total data variance. This elemental grouping is relatively and positively loaded with lithophile elements with respect to the LREE and HREE. The significant loading suggests REE fractionation in the study area that involved both the LREEs and HREEs. The strong loading of Ho (0.616), Er (0.609), Tm (0.659), Yb (0.747) and Lu (0.828) establishes their mutual relationship as HREEs. Factor 2 (La, Ce, Pr, Nd, Eu, Gd, Tb, Dy, Ho, Er, Tm) account for 0.336% of the total variance. The strong loading of La (0.637), Ce (0.64), Pr (0.63), Nd (0.632) reflects their association as LREEs while the strong loading of Gd (0.627), Tb (0.64) and Dy (0.623) indicates their relationship as MREEs. Factor 3 (La, Ce, Pr, Nd, Sm, Eu, Gd, Tb, Dy, Ho, Er) account for 0.29% of the total variance, and Sm (0.805) is strongly loaded. Factor 4 and Factor 5 are not loaded and they account for 0.007 and 0.003% of the total data variance respectively. The communality values range from 0,996 to 1 (Table 4) and indicate a common variance.

TABLE III Pearson's Correlations between Ree Concentrations

	La	Ce	Pr	Nd	Sm	Eu	Gd	Tb	Dy	Ho	Er	Tm	Yb	Lu
La	1													
Ce	0.9998	1												
Pr	0.9995	0.9997	1											
Nd	0.9995	0.9998	0.9998	1										
Sm	0.9347	0.9329	0.9366	0.9351	1									
Eu	0.9934	0.9934	0.9943	0.9937	0.9344	1								
Gd	0.9985	0.9990	0.9990	0.9989	0.9349	0.9929	1							

Tb	0.9975	0.9980	0.9975	0.9974	0.9256	0.9909	0.9992	1						
Dy	0.9957	0.9965	0.9964	0.9962	0.9241	0.9932	0.9983	0.9990	1					
Ho	0.9910	0.9920	0.9924	0.9921	0.9120	0.9936	0.9945	0.9956	0.9982	1				
Er	0.9768	0.9778	0.9800	0.9801	0.9260	0.9817	0.9818	0.9803	0.9822	0.9833	1			
Tm	0.9808	0.9816	0.9814	0.9818	0.8885	0.9883	0.9837	0.9856	0.9895	0.9945	0.9789	1		
Yb	0.9508	0.9522	0.9543	0.9537	0.8662	0.9733	0.9569	0.9571	0.9661	0.9780	0.9716	0.9847	1	
Lu	0.9144	0.9149	0.9149	0.9159	0.8235	0.9322	0.9195	0.9207	0.9284	0.9397	0.9281	0.9507	0.9709	1

TABLE IV Varimax Rotated Factor Loading and Communalities

Variable	Factor 1	Factor 2	Factor 3	Factor 4	Factor 5	Communality
La	0.541	0.637	0.547	-0.04	0.006	0.999
Ce	0.543	0.64	0.542	-0.046	0.007	1
Pr	0.544	0.63	0.55	-0.054	0.015	0.999
Nd	0.545	0.632	0.547	-0.055	0.007	0.999
Sm	0.413	0.423	0.805	-0.042	0.024	1
Eu	0.596	0.579	0.547	-0.044	0.084	0.998
Gd	0.553	0.627	0.544	-0.063	0.006	1
Tb	0.559	0.64	0.523	-0.065	0.004	0.999
Dy	0.58	0.623	0.518	-0.065	0.029	0.998
Ho	0.616	0.607	0.492	-0.073	0.057	0.998
Er	0.609	0.533	0.546	-0.214	0.017	1
Tm	0.659	0.59	0.448	-0.078	0.082	0.996
Yb	0.747	0.48	0.432	-0.108	0.113	0.999
Lu	0.828	0.397	0.391	0.004	-0.058	1
Variance	5.0881	4.7057	4.0601	0.0948	0.0352	13.984
% Var	0.363	0.336	0.29	0.007	0.003	0.999
Cum %	0.363	0.699	0,989	0,996	0,999	1,998

4.3.3. Principal Component Analysis (PCA)

PCA (Table 5) results in five components that explain 100% of the total variance (eigenvalue) for the studied samples. The first component (PC1) that accounts for 100% of the total variance contains Ce (0.802), this element is strongly loaded reflecting high Ce enrichment relative to the other REEs. The second (PC2), third (PC3), fourth (PC4) and fifth (PC5) components accounting for 0% of the total variance respectively. The component plot (Fig. 4) obtained after component analyses show the placement of elements in three major principal components (PC1, PC2, PC3), in which elements scattering in the rotated space displaying their mutual association.

TABLE V ROTATED COMPONENT MATRIX

Variable	PC1	PC2	PC3	PC4	PC5
La	0.397	0.074	-0.726	-0.536	-0.111
Ce	0.852	0.199	0.129	0.446	0.112
Pr	0.09	-0.147	0.082	0.011	-0.798
Nd	0.327	-0.513	0.54	-0.56	0.105
Sm	0.021	-0.818	-0.39	0.405	0.109
Eu	0.001	-0.003	0	-0.004	-0.041
Gd	0.031	-0.031	0.057	0.175	-0.387
Tb	0.003	0.006	0.004	0.016	-0.052
Dy	0.011	0.013	0.041	0.068	-0.335
Ho	0.001	0.003	0.009	0.004	-0.075
Er	0.003	-0.028	0.025	-0.021	-0.171
Tm	0	0.001	0.002	-0.002	-0.013
Yb	0.001	0.001	0.014	-0.011	-0.121
Lu	0	0	0.001	-0.002	-0.009
Eigenvalue	1292271	96	88	23	3
% Var	100	0	0	0	0
Cum %	100	100	100	100	100

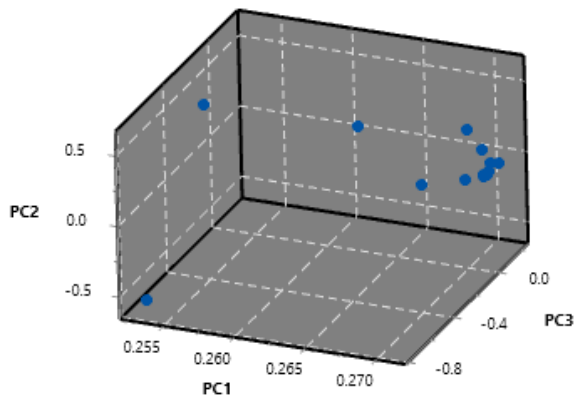

Figure4. Principal Component Diagram

5. Upper background threshold (UBT)

The upper background threshold (UBT) values are calculated for the REEs and the values are presented in Tables 2. The UBT is the upper limit of element concentration above which the element is considered anomalous. Most of the REEs calculated fall below the background values (Table 1, 2) except LREEs such as La (samples EB02 to EB015), Ce, Pr (samples EB02, EB04 to EB008, EB14 and EB15), Nd (samples EB02 to EB09, EB11 to EB15), and Ga (samples EB05 to EB07) that fall above the UBT.

6. Discussion

6.1. Lanthanide Concentrations

Lanthanides are lithophile refractory elements and their relative proportions in the silicate earth are identical to the proportions found in the carbonaceous chondrites [6].

The studied lanthanides have Ce, La, Nd, Pr enrichment and the proportion enrichment of REEs in the study area is still remained similar with increasing atomic number. The order of the average concentrations of REEs in the study area is different to the Oddo-Harkins rule [46], [47] that is Ce > La > Nd > Pr > Sm > Gd > Dy > Er > Yb > Eu > Tb > Ho > Tm > Lu. Lanthanide concentrations from Bwanebwa area is also different to the order of magnitude as that in the earth's crust [8], in the upper continental crust [9], South China Sea [48], mean REE values in oceanic crust [49], Redang Island Marine Sediment in Terengganu Coastal Waters [50], Bayan Obo ores [51] and Edéa area [27] situated within the Nyong Series in Cameroon. These observations show that REEs set up a complex group [52] and [27].

6.2. REE Differentiation Patterns

Crust normalized REE patterns were used to evaluate REEs fractionation. Accordingly, the chondrite-normalized REE distribution patterns for the studied stream sediments are generally identical, indicating the consistency of geochemical distribution of REEs in stream sediments. The curves of the REE patterns extend downward from left to right characterizing the LREEs enrichment and HREEs depletion. The ratio of La_N/Yb_N quantifies the inclination of the normalized REE curves. This ratio of La_N/Yb_N (11.74-27.93) is greater than 1, the curves of LREE incline to right side, meaning that the stream sediments is rich in LREEs and low in HREEs. The enrichment patterns of LREEs in the studied stream sediments is due to the fact that HREEs are more soluble and more complex than middle or light REE and are more strongly absorbed on most substrates [53] and [27]. Generally, higher concentrations of LREE are observed in soils that developed on phosphate and carbonate rocks, whereas the basalt-weathered soils show enrichment in HREE [54]. The average values, solely for LREEs (616.49 ppm) and Gd (68.88 ppm) are higher than those reported in the UCC: LREEs = 27.86 ppm; Gd = 4.66 ppm [55].These average values are also higher than those reported by [56] in Brazil.

6.3. Ce and Eu anomalies

A very slightly positive Ce anomaly (Ce/Ce* = 1.04-1.07) and a strong negative Eu anomaly (Eu/Eu* = 0.097-0.17) were observed, indicating that differentiation occurred between Ce, Eu and other lanthanides. The depletion or enrichment of Ce and Eu usually occurs in the natural environment, which may be linked to their oxidation state and mobility under different oxidation-reduction conditions [57]. Ce of both oxidation states are found in soils, but under redox conditions Ce^{3+} is more easily oxidized to Ce^{4+} with higher oxygen fugacity and is much less mobile resulting in positive Ce anomaly (Ce/Ce* > 1). In addition, the positive Ce anomaly recorded in the study area represents an enrichment of Ce compared with its neighboring elements. Chen et al. (2007) reported that varying degrees of positive Ce anomaly was shown in red soils from southern China, which reflected the differentiation of Ce caused by different oxidation environments during the process of soil-forming. Eu is an incompatible element in the trivalent form (Eu^{3+}) in an oxidizing magma, but is preferentially incorporated into plagioclase in its divalent form (Eu^{2+}) in a reducing magma. This ion-exchange process is the basis of the negative Eu anomaly (Eu/Eu* < 1).

6.4. Geochemical Parameters

The properties of REE composition and differentiation patterns are not influenced by weathering, transportation process, sedimentation and diagenesis. Meanwhile the provenance information carried by REE remains essentially unchanged, and consequently REEs could be used as a provenance indicator in the geochemical studies [59]. The binary cross-correlation plots of various geochemical parameters were used to discriminate natural variation in REE concentrations from other sources which would influence REE levels. The cross-plots between total REEs and REEs differentiation characteristics, such as LREE/HREE ratio, Eu anomaly and Ce anomaly were shown in Fig. 5. The geochemical parameters of REE composition from the present study exhibit a wide range of variability. The stream sediment samples from Bwanebwa area displayed high LREE/HREE ratios, distinct negative Eu anomalies and very weak positive Ce anomalies when compared with the fluvial sediments and REE minerals which influenced by the original source of REEs and significantly enhanced by the bare tailings [42]. Wang et al. (2011) and Xie et al. (2014) demonstrated that fine grain size may contribute to the enrichment of the REE abundance. There have also been reports suggesting that a positive correlation existed between the REE differentiation and the gradation of the dust grain size [60]. These results confirmed that the REE distribution characters reflected the compositions of materials in the source regions, but are also influenced by weathering and pedogenesis. It is worthy to note that soil properties such as clay minerals, organic matter, Fe content, carbonate, and pH play key roles for the distribution of REEs [61].

6.5. REE Distribution and Origin

The concentration of REEs in the study area ranged from 0.1 to 3758 mg/kg with a mean value of 272.2 mg/kg. Therefore the measured mean REEs levels in the stream sediment samples were higher than the background values of REEs in soil of Baotou region [62]. Result observed for the sum of all REEs (ΣREE =1471.56-7674.2 mg/kg, av. = 3811 mg/kg) in the present study was also higher than that reported in soil (181 mg/kg) by [26], in Japan (98 mg/kg) [63], Australia (105 mg/kg) [64] and Germany (305 mg/kg) [65]. LREEs (La, Ce, Pr, Nd) and Ga fall above the UBT limit and are considered as anomalous. A five-factor model of the REEs that accounts for 1.998% of the total data cumulative variance has been recorded in the study area and the significant loading of factors suggests REE fractionation. The communality values vary from 0,996 to 1, with a higher value reflecting stronger community structure. Factor 1,

factor 2 and factor 3 are more important than factor 4 and factor 5. The correlation matrix has shown an unusually case where REEs correlated higher positively with their respective correspondents. These findings confirm the aforementioned results and provide evidence for similar input sources and common geochemical characteristics of the elements. Therefore, lanthanide concentrations in the study area were of geogenic origins and not influenced by anthropogenic sources. The abundance of REEs in Bwanebwa area is related to the lithology made up of granites and associated pegmatites. Since lanthanides in stream sediments are mobile, they can continuously accumulate in stream various pathways such as atmospheric deposition [1], mining activities [66] and application of REE fertilizers [67].

Cerium shows the highest average content of REEs, followed by La, Nd, Pr, Gd and Sm. This result can be observed in the boxplot (Fig. 6) were the median value of Ce is 1792 mg/kg with the range of 703 to 3758 mg/kg, La (835 mg/kg; range: 333-1753 mg/kg), Nd (704 mg/kg; range: 270-1441 mg/kg), Pr (191 mg/kg; range: 76.1-392 mg/kg), Gd (66.8 mg/kg; range: 27.1-138 mg/kg). Therefore, patterns of Ce distribution show higher than the other lanthanides. The REE fractions of these profiles also showed an enrichment of LREE relative to the HREE (Fig. 6). These results indicate that the REEs patterns of the stream sediment samples around Bwanebwa area are consistent with those of Bayan Obo ores [51]. Therefore, the results of this work serve as guide for lanthanides exploration in Bwanebwa.

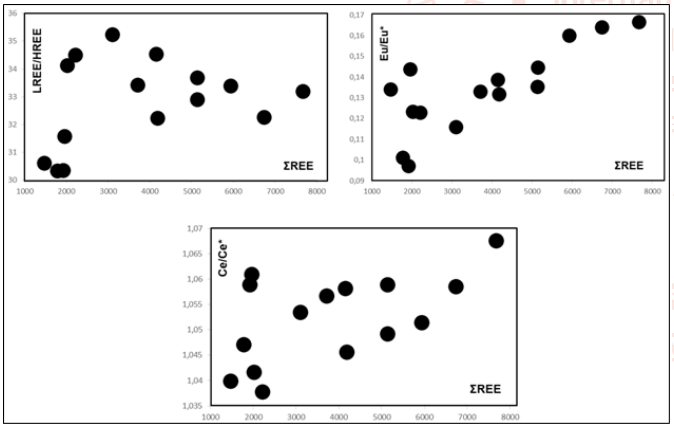

Figure5. Cross-correlation plots of various geochemical parameters for REEs

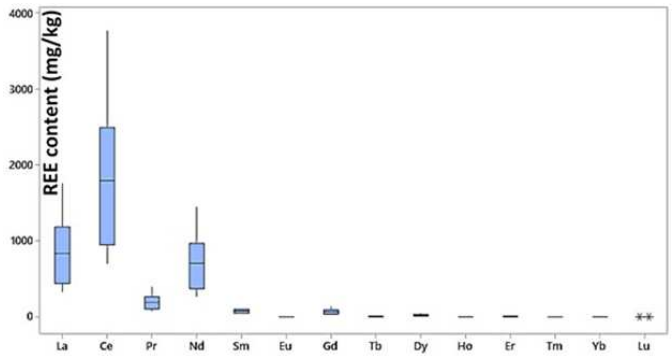

Figure6. Boxplot of rare earth elements from Bwanebwa area

7. CONCLUSION

Largely distributed around Bwanebwa area, the chemical analyses revealed a wide variability of lanthanide concentrations with ΣREE = 1471.56-7674.2 ppm (av. = 3811 ppm) showing a normal distribution pattern. Lanthanides show a high enrichment in La (332-1750 ppm, av. = of 863.8 ppm), Ce (703-3758 ppm, av. = 1846.93 ppm), Pr (76.11-392 ppm, av. = 196.89 ppm) and Nd (269-1440 ppm, av. = 715.53 ppm), and the proportion enrichment of REEs in the study area is still remained similar with increasing atomic number. The order of the average concentrations of REEs in stream sediments around Bwanebwa area is Ce > La > Nd > Pr > Sm > Gd > Dy > Er > Tb > Ho >Yb > Eu > Tm > Lu, which was different to that found in the Oddo-Harkins rule (Ce > La > Nd > Pr > Sm > Gd > Dy > Er > Yb > Eu > Tb > Ho > Tm > Lu), earth's crust, upper continental crust, South China Sea, mean REE values in oceanic crust, Redang Island Marine Sediment in Terengganu Coastal Waters, Bayan Obo ores, Edéa (Nyong Series), suggesting that REEs set up a complex group.

The LREE/HREE ratio (31.57-35.24, av. = 32.82) showed that the content of LREE (1425-7449.8, av. = 3699) is significantly higher than that of HREE (46.56-224.4, av. 112.07). The LREEs account for 97.06% of the total REEs, this percentage is in agreement with the trend that was observed in the earth's crust and in the Bayan Obo ores. Chondrite-normalized REE distribution patterns are generally identical, indicating the consistency of geochemical distribution of REEs in stream sediments. Patterns are strongly fractionated (La_N/Yb_N = 11.22-17.92), with LREEs significantly fractionated (La_N/Yb_N of 11.74-27.93) relative to HREEs (Gd_N/Yb_N = 7.40-16.69, av. = 13.35), implying that HREEs are more soluble and more complex than middle or light REE and are more strongly absorbed on most substrates. Slightly positive Ce anomaly (Ce/Ce* = 1.04-1.07) and strong negative Eu anomaly (Eu/Eu* = 0.097-0.17) were observed, indicating that differentiation occurred between Ce, Eu and other lanthanides. Therefore the positive Ce anomaly recorded represents an enrichment of Ce compared with its neighboring elements.

A five-factor model of the REEs that accounts for 1.998% of the total data cumulative variance have been observed, with the communality values (0,996-1) reflecting stronger community structure. PCA results in five components that explain 100% of the total variance (eigenvalue), with the placement of elements in three major principal components, in which elements scattering in the rotated space displaying their mutual association. The results provide evidence for similar input sources and common geochemical characteristics of REEs. Therefore, lanthanide concentrations in the study area were of geogenic origins and not influenced by anthropogenic sources. The abundance of REEs is related to the lithology made up of granites and associated pegmatites. Cerium shows the highest average content of REEs, followed by La, Nd, Pr, Gd and Sm, hence pattern of Ce distribution shows higher than the other lanthanides. LREEs (La, Ce, Pr, Nd) and Ga fall above the UBT limit and are considered as anomalous. Therefore, the results of this work serve as guide for lanthanides exploration in Bwanebwa area.

References

[1] G. Tyler, "Rare earth elements in soil and plant systems-A review," Plant Soil, vol. 267, pp. 191–206, 2004.

[2] P. Henderson, "Rare earth element geochemistry Developments, in Geochemistry," 2th Eds. Amsterdam: Elsevier, 1984, 510p

[3] C. Laveuf, & S. Cornu, "A review on the potentiality of rare earth elements to trace pedogenetic processes," Geoderma, vol. 154, pp. 1–12, 2009.

[4] L. V. Perelomov, "Interaction of RareEarth Elements with Biotic and Abiotic Soil Components," Agrokhimiya, No. 11, pp. 85–96, 2007.

[5] V. M. Goldschmidt, T. Barth, G. Lunde, "Geochemische Verteilungsgesetze der Elemente. 5, Isomorphie und Polymorphie der Sesquioxyde," Die Lanthaniden Kontraktion und ihre Konsequenzen, *Jacob Dybwad: Oslo*, Norway (In German), 1925.

[6] F. Bea, "Geochemistry of the Lanthanide Elements," [XXXV Reunión de la Sociedad Española de Mineralogía, Department of Mineralogy and Petrology, University of Granada pp. 1-12, 2015]

[7] A. Jordens, Y.P. Cheng, & K.E. Waters, "A review of the benefciation of rare earth element bearing minerals," Miner Eng, vol. 41, pp. 97–114, 2013.

[8] S. R. Taylor & S. M. McLennan, "The geochemical evolution of the continental crust," Reviews of Geophysics, vol. 33, pp. 241–265, 1995.

[9] R. L. Rudnick & S. Gao, "Composition of the continental crust," Treatise on geochemistry, vol. 3, pp. 1–64, 2003.

[10] S. M McLennan, "Rare earth elements in sedimentary rocks: influence of the provenance and sedimentary process," Rev. Mineral. Vol. 21, pp. 169-200, 1989.

[11] J. Gaillardet, Géochimie comparée de deux grands systèmes fluviaux tropicaux: le Congo et l'Amazone. Géochimie isotopique du bore dans les coraux. Thesis, Univ. Pierre-et-Marie-Curie, Paris-6, France, 1995, 427 pp.

[12] A. P. Jones, F. Wall and C. T. Williams, "Rare Earth Minerals Chemistry, Origin and Ore Deposits Series: The Mineralogical Society Series," Springer Publisher, Vol. 7, 1996.

[13] B. Dupre, J. Gaillardet, D. Rousseau and C. Allegre, "Major and trace elements of river-borne material: the Congo Basin," Geochim. Cosmochim. Acta, vol. 60, pp. 1301-l321, 1996.

[14] S. A. Wood, "The aqueous geochemistry of rare-earth elements and yttrium," Chem. Geol. Vol. 82, pp. 159-l 86, 1990.

[15] M. A. Kimoto, X. C. Nearing, D. Zhang, M. Powell, "Applicability of Rare Earth Element Oxides as a Sediment Tracer for Coarse-Textured Soils," Catena, Vol. 65, No. 3, pp. 214-221, 2006. doi:10.1016/j.catena.2005.10.002

[16] K. Binnemans, P. T. Jones, "Rare Earths and the Balance Problem," J. Sustain. Metall. Vol. 1, pp. 29–38, 2015. [CrossRef]

[17] K. M. Goodenough, F. Wall, D. Merriman, "The Rare Earth Elements: Demand, Global Resources, and Challenges for Resourcing Future Generations," Nat. Resource. Res. vol. 27, pp. 201–216, 2018. [CrossRef]

[18] A. R. Chakhmouradian, F. Wall, "Rare Earth Elements: Minerals, Mines, Magnets (and More)," Elements vol. 8, pp. 333–340, 2012. [CrossRef]

[19] K. M. Goodenough, J. Schilling, E. Jonsson, P. Kalvig, N. Charles, J. Tuduri, E. A. Deady, M. Sadeghi, H. Schiellerup, A. Müller, "Europe's rare earth element resource potential: An overview of REE metallogenetic provinces and their geodynamic setting," Ore Geol. Rev. vol. 72, pp. 838–856, 2016. [CrossRef]

[20] U. S. Geological Survey, "Mineral commodity summaries 2013," 2014, 196p.

[21] N. K. Foley, "Rare Earth Elements: The role of geology, exploration, and analytical geochemistry in ensuring diverse sources of supply and a globally sustainable resource," J. Geochem. Explor, vol. 133, pp. 1-5, 2013.

[22] DNPM (Departamento Nacional de Produção Mineral). "Terras raras," 2010. http://www.dnpm.gov.br/assets/galeriadocumento/sumariomineral2004/TERRAS%20RARAS%202004.pdf (last search 03.05.2013)

[23] M. Sadeghi, P. Petrosino, A. Ladenberger, S. Albanese, M. Andersson, G. Morris, A.M. Lima, B. De Vivo and the GEMAS Project Team, "Ce, La and Y concentrations in agricultural and grazing-land soils of Europe," J. Geochem. Explor, vol. 133, pp. 202-213, 2013.

[24] Anonymous, "Situation and Policy of China's Rare Earth Industry, White Paper (English Version). The State Council Information Office of the People's Republic of China," 2014. (http://www.scio.gov.cn/zfps/ndhf/2012/Document/1175419/1175419.htm) (2012) Date of access: 01/12/2014.

[25] Z. Chen, "Global rare earth resources and scenarios of future rare earth industry," J.Rare Earths vol. 29, pp. 1–6, 2011.

[26] Z. Y. Hu, S. Haneklaus, G. Sparovek & E. Schnug, "Rare earth elements in soils. Commun," Soil Sci. Plant Anal. Vol. 37, pp. 1381–1420, 2006.

[27] J. L Ndema Mbongué, C. Sigué, J.P Nzenti, E. Suh Cheo, "Distribution of Rare Earth Elements in the Metamorphic Rocks of the Paleoproterozoic Nyong Unit (Congo Craton, South – Cameroon)," IJRDO - Journal of Applied Science; vol. 5; Issue 7, pp. 35-49, July 2019.

[28] C. Castaing, J. L. Feybesse, D. Thieblemont, C. Triboulet, and P. Chevremont, "Palaeogeographical reconstructions of the Pan-African/Brasiliano orogen: closure of an oceanic domain or intracontinental convergence between major blocks," Prec Res. vol. 69, pp. 327-344, 1994.

[29] S. P. Neves, J. M. R. Silva & G., Mariano, "Oblique lineations in orthogneisses and supracrustal rocks: vertical partitioning of strain in a hot crust (eastern Borborema Province, NE Brazil)," J. Struct Geol. Vol. 27, pp.1507-1521, 2005.

[30] J. P. Nzenti, P. Barbey, J. Macaudiere and D. Soba, "Origin and evolution of the late Precambrian high-grade Yaounde gneisses (Cameroon)," Prec Res. vol. 38, pp. 91-109, 1988.

[31] J. P. Nzenti, P. Barbey, J. M. L. Bertrand et J. Macaudière, "La chaîne panafricaine au Cameroun : cherchons suture et modèle,". In S. G. F. Eds., 15e réunion des Sciences de la Terre, Nancy, France, 1994, 99p

[32] J. P. Nzenti, P. Barbey, F. M. Tchoua, "Evolution crustale au Cameroun: éléments pour un modèle géodynamique de l'orogenèse néoproterozoïque,". In Géologie et environnements au Cameroun, Vicat et Bilong editors, collection GEOCAM. *2*, 1999, pp. 397-407

[33] JP. Nzenti, B. Kapajika, G. Wörner and R.T. Lubala, "Synkinematic emplacement of granitoids in a Pan-African shear zone in Central Cameroon," J. Afr. Earth Sci. vol. 45, pp. 74-86, 2006.

[34] T. Ngnotué, J.P. Nzenti, P. Barbey and F.M. Tchoua, "The Ntui-Betamba high-grade gneisses: a Northward extension of the Pan-African Yaounde gneisses in Cameroon," J. Afr. Earth Sci. vol. 31, pp. 369-381, 2000.

[35] T. Ngnotué, S. Ganno, J.P. Nzenti, B. Schulz, D. Tchaptchet Tchato, E. Suh Cheo, "Geochemistry and geochronology of Peraluminous High-K granitic leucosomes of Yaoundé series (Cameroon): evidence for a unique Pan-African magmatism and melting event in North Equatorial Fold Belt," Int. J. Geosci. 3, 525-548, 2012.

[36] E. L. Tanko Njiosseu, Géologie de la reégion de Tonga dans la partie Sud du domaine centre de la chaîne au Cameroun: évolution métamorphique, géochimie et géochronologie. Th. Doct Ph/D, Univ. Ydé I, 2012.

[37] B. Kankeu, R. O. Greiling, J. P. Nzenti, S. Ganno, P.Y.E. Danguene, J. Bassahak, J. V. Hell, "Contrasting Pan-African structural styles at the NW margin of the Congo Shield in Cameroon," J. Afr. Earth Sci. 2017. http://dx.doi.org/10.1016/j.jafrearsci.2017.06.002.

[38] J. P. Nzenti, "Neoproterozoic alkaline metamorphic igneous rocks from the Pan-african North Equatorial fold belt (Yaoundé, Cameroon): biotites and magnetite rich pyroxenites," J. Afr. Earth Sci. vol. (26) 1, pp 37-47, 1998.

[39] S. F. Toteu, W. R. Van Schmus, J. Penaye, A. Michard, "New U-Pb and Sm–Nd data from north-central Cameroon and its bearing on the pre-PanAfrican history of Central Africa," Precambr. Res. 108, pp. 45–73, 2001.

[40] B. Kankeu, R. O. Greiling, J. P. Nzenti, "Pan-African strike-slip tectonics in eastern Cameroon-Magnetic fabrics (AMS) and structure in the Lom basin and its gneissic basement (Bétare-Oya area)," Prec. Res. vol. 17(3-4), pp. 258-272, 2009.

[41] B. Kankeu, O. Reinhard Greiling, J. P Nzenti, J. Bassahak and J. V Hell, "Strain partitioning along the Neoproterozoic Central Africa Shear Zone system: structures and magnetic fabrics (AMS) from the Meiganga area, Cameroon," N. Jb. Geol. Paläont. Abh. vol. 265/1, pp. 27–47, 2012.

[42] L. Wang, T. Liang, "Geochemical fractions of rare earth elements in soil around a mine tailing in Baotou, China," Sci. Rep. 5:12483, pp. 1-11, 2015.

[43] D. McGrath, C. Zhang & O. T. Carton, "Geostatistical analyses and hazard assessment on soil lead in silvermines area, Ireland," Environ. Pollut, vol. 127, pp. 239–248, 2004.

[44] S. Karanlik, N. Aqca, & M. Yalcin, "Spatial distribution of heavy metals content in soils of Amik plain (Hatay, Turkey)," Environ. MonitAssess, vol. 173, pp. 181–191, 2011.

[45] J. C. Davis, Statistics and data analysis in Geology, 2nd ed., Wiley, New York 1973.

[46] L. Wang, T. Liang, Q. Zhang & K. Li, "Rare earth element components in atmospheric particulates in the Bayan Obo mine region," Environ. Res. vol. 31, pp. 64–70, 2014.

[47] R. A. Sutherland, "Bed sediment-associated trace metals in an urban stream, Oahu, Hawaii," Environ. Geol. vol. 39, pp. 611-27, 2000.

[48] G. Bao and Q. Li, "Geochemistry of Rare Earth Elements in Ferromanganese Nodules (Crusts) of the South China Sea," Oceanologia et Limnologia Sinica, vol. 24, No. 3, pp. 304-309, 1993.

[49] A. B. Ronov, Y. A. Balashov and Y. P. Girin, "Regularities of Rare Earth Element Distribution in the Sedimentary Shell and in the Crust of the Earth," Sedimentology, vol. 21, pp. 171-193, 1974. doi:10.1111/j.1365-3091.1974.tb02055.x

[50] A. Nor Antonina, N. A. M. Shazili, B. Y. Kamaruzzaman, M.C. Ong, Y. Rosnan, F.N. Sharifah, "Geochemistry of the Rare Earth Elements (REE) Distribution in Terengganu Coastal Waters: A Study Case from Redang Island Marine Sediment," Open Journal of Marine Science, vol. 3, pp. 154-159, 2013.

[51] C. Xu, R. N. Taylor & W. Li, "Comparison of fluorite geochemistry from REE deposits in the Panxi region and Bayan Obo, China," J. Asian Earth Sci. vol. 57, pp. 76–89, 2012.

[52] [52] B. Hamid, C. Abdelmajid, C.E. Rajaa, K.H. Oum, C. Said; "Distribution of the rare earth elements in the sediments of the Bouregreg river (Morocco) using the instrumental neutron activation analysis (INAA)," J. Appl. Sci. Environ. Manage, vol. 11 (1), pp. 57 – 60, 2007.

[53] R. H. Byrne and K. H. Kim, "Rare Earth Precipitation and Co-Precipitation Behavior: The Limiting Role of on PO4-3 on Dissolved Rare Earth Concentrations in Seawater," Geochimica Cosmochimica Acta, Vol. 57, No. 3, pp. 519-526, 1993. doi:10.1016/0016-7037(93)90364-3

[54] J. Rinklebe, C. Franke & H.-U. Neue, "Aggregation of floodplain soils based on classifcation principles to predict concentrations of nutrients and pollutants," Geoderma 141, pp. 210–223, 2007.

[55] S. R. Taylor, S. M. McLennan, The continental crust: its composition and evolution. Blackwell Publishing, Oxford, UK, 1985, pp. 312

[56] D. V. Pérez, A. M. F. C. Saldanh, N. A. Meneguelli, J. C. Moreira, D. S. Vaitsman, "Geoquímica de alguns solos brasileiros," Embrapa Solos, Rio de Janeiro, vol. 4, pp. 1-14, 1997.

[57] X. Cao, X. Wang & G. Zhao, "Assessment of the bioavailability of rare earth elements in soils by chemical fractionation and multiple regression analysis," Chemosphere vol. 40, pp. 23–28, 2000.

[58] B. Chen, H. Wei, Z. Huang, Y. Zhou, "Cerium Anomalies in Supergene Geological Bodies and Its Effecting Factors," Chin. Rare Earths, vol. 28, pp. 79–83, 2007.

[59] L. Wang, T. Liang, P. A. Kleinman, et al, "An experimental study on using rare earth elements to trace phosphorous losses from nonpoint sources," Chemosphere vol. 85, pp. 1075–1079, 2011.

[60] Y. Xie, J. Meng & L. Guo, "REE geochemistry of modern eolian dust deposits in Harbin city, Heilongjiang province, China: Implications for provenance," Catena vol. 123, pp. 70–78, 2014.

[61] Q. Zhang, G. Han, M. Liu and L. Wang, "Geochemical Characteristics of Rare Earth Elements in Soils from Puding Karst Critical Zone Observatory, Southwest China," Sustainability, Vol. 11, 4963; pp. 2-14, 2009. doi: 10.3390/su11184963

[62] CNEMC (China National Environmental Monitoring Center). "The Background Concentrations of Soil Elements in China," Chinese Environment Science Press, Beijing, 1990.

[63] S. Yoshida, Y. Muramatsu, K. Tagami, et al, "Concentrations of lanthanide elements, Th, and U in 77 Japanese surface soils," Environ. Int. vol. 24, pp. 275–286, 1998.

[64] E. Diatloff, C.J. Asher & F.W. Smith, "Concentrations of rare earth elements in some Australian soils," Aust. J. Soil Res. vol. 34, pp. 735–747, 1996.

[65] M. Loell, C. Albrecht & P. Felix-Henningsen, "Rare earth elements and relation between their potential bioavailability and soil properties, Nidda catchment (Central Germany)," Plant Soil vol. 349, pp. 303–317, 2011.

[66] H. Zhang, J. Feng & W. F. Zhu, "Rare earth element distribution characteristics of biological chains in rare earth element–high background regions and their implications," Biol. Trace Elem. Res. vol. 73, pp. 19–27, 2000.

[67] X. Pan, D.C. Li & A. Peng, "Application of rare-earth elements in the agriculture of China and its environmental behavior in soil," Environ. Sci. Pollut. R. vol. 9, pp. 143–148, 2002.